How much of a bubble is there in 184Hg?

Nilsson, Sven Gösta; Nix, J R; Möller, P

Published in:
Nuclear Physics, Section A

1974

F:510

Nuclear Physics **A222** (1974) 221–234; © *North-Holland Publishing Co., Amsterdam*

HOW MUCH OF A BUBBLE IS THERE IN ^{184}Hg?

S. G. NILSSON †, J. R. NIX and P. MÖLLER †
Los Alamos Scientific Laboratory, University of California
Los Alamos, New Mexico 87544 ††

and

I. RAGNARSSON
Nordita, Copenhagen, Denmark

Received 1 August 1973
(Revised 17 December 1973)

Abstract: Recent suggestions of the existence of bubble-shape nuclei are examined for a few selected nuclei in terms of a Strutinsky shell-correction method type of calculation, based on the folded-Yukawa model. The inner surface is treated by a modified version of the liquid-drop model, allowing for the finite range of the nuclear diffuseness and nucleon-nucleon interaction. It appears safe to conclude that ^{184}Hg is not bubble-like. The observed large $\langle r^2 \rangle$ in this region of Hg nuclei is explained as being associated with a change in distortion. This change is shown to be largely an effect of the introduction of quadrupole pairing.

1. Introduction

Recently Wong [1]) reexamined an idea put forth by Wheeler [2]) and Swiatecki [3]) that nuclei, in order to decrease the Coulomb repulsion, may assume bubble shapes. In the presently accessible region of nuclei there may not exist a case with an actual vacuum in the center of the nucleus; on the other hand, recent Hartree-Fock calculations by Davies, Krieger and Wong, and by Campi and Sprung [4]) give strong evidence for a thinning-out of nuclear matter in the center of a few specific nuclei to an extent where the bubble concept is reasonably applicable.

In ref. [1]) Wong generated a wine-bottle potential with a radial harmonic oscillator potential centered midway between the inner and outer radii. The radii are denoted by R_1 and R_2, respectively. Wong subsequently studied the single-particle levels as functions of R_1/R_2. For small displacements the neutron gaps 82 and 126 were found to be replaced by 80 and 120, while for larger displacements the neutron numbers 104 and 146 were found to correspond to dominant gaps. A Strutinsky type calculation with inclusion of the surface energy of the interior surface, in addition to the Coulomb energy and the surface energy of the outer surface, was then carried out for the total energy as a function of the radial shape. Only purely spherical shapes were considered. From these calculations Wong found that a bubble should form in

† On leave from the Lund Institute of Technology, Lund, Sweden.
†† Supported by the US Atomic Energy Commission and the Swedish Atomic Research Council.

April 1974

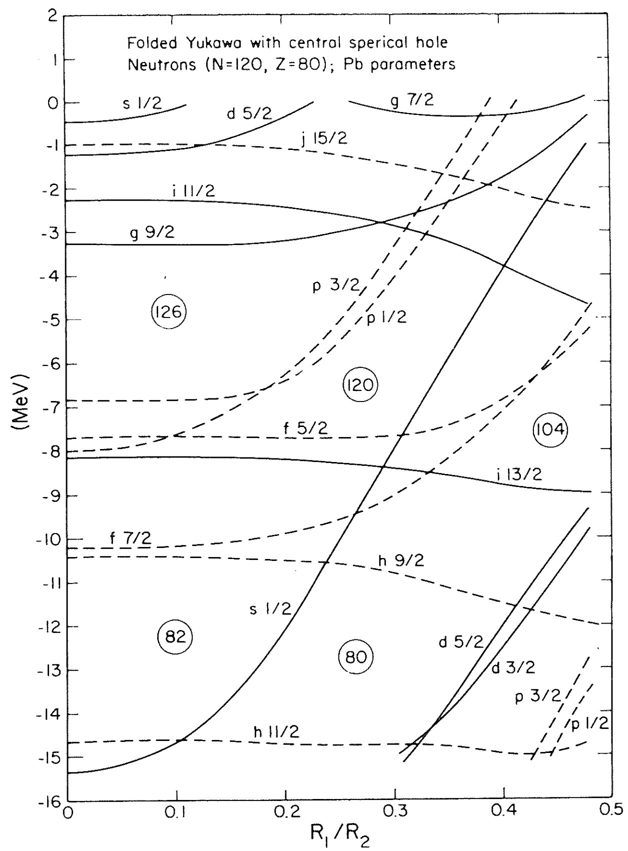

Fig. 1. Single-neutron levels as functions of R_1/R_2, where R_1 and R_2 are the inner and outer bubble radii of the uniform sharp-surface generating potential for the folded-Yukawa potential. Note the shells at $N = 120$ and $N = 104$.

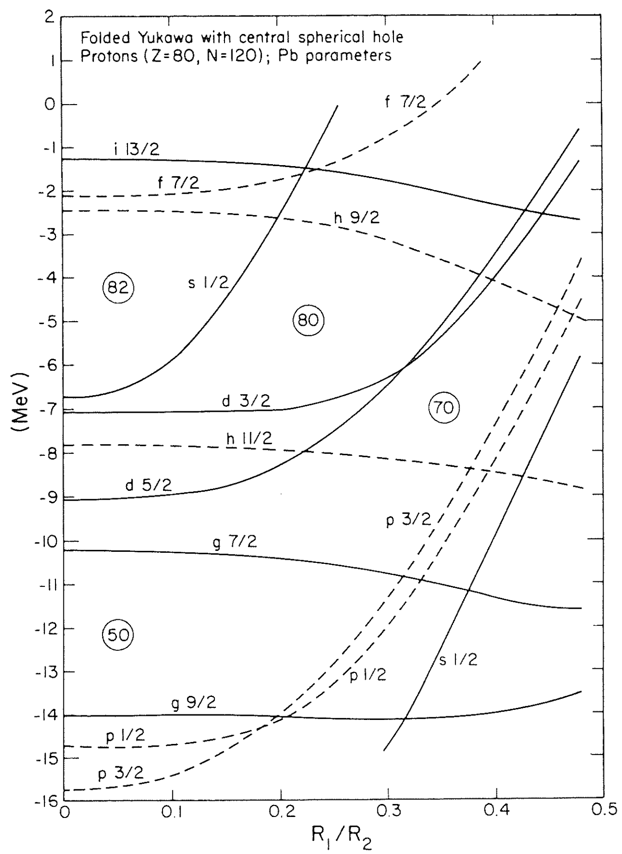

Fig. 2. Analogous to fig. 1 but for proton orbitals.

the ^{200}Hg case, with $R_1/R_2 \approx 0.07$. No specific calculation was carried out by Wong for ^{184}Hg, as $Z = 80$ and $N = 104$ occur as energy gaps for very different bubble distortions. This finding by Wong is confirmed in the present calculations (see figs. 1 and 2). In fact, the neutron and proton contributions are seen to be out of phase in terms of R_1/R_2, as discussed in the following.

From optical pumping experiments Bonn *et al.* [5]) observed an increase of 2.1–2.5 % in $\langle r^2 \rangle$ from ^{187}Hg on the one hand, to ^{185}Hg, ^{183}Hg, and, most recently, ^{181}Hg, on the other hand. As the authors of ref. [6]) point out, if this increase were interpreted as a change in nuclear radius but not angular shape, it would imply the same volume for ^{183,185}Hg as for ^{196}Hg. The most near-lying explanation involves, of course, not a change in radius, but a change in spheroidal deformation. This

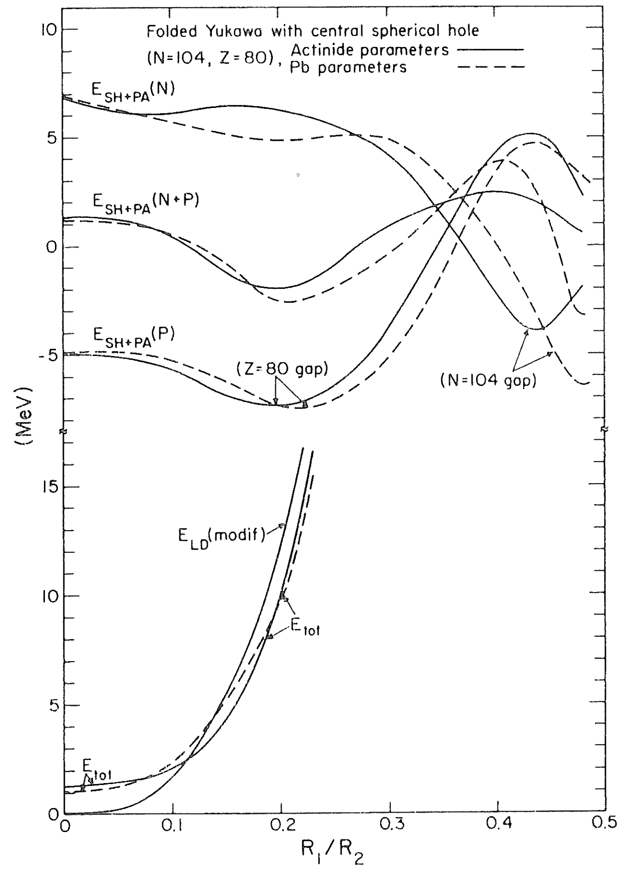

Fig. 3. The sum of shell and pairing energies as functions of R_1/R_2 for neutrons (N), protons (P), and neutrons+protons (N+P). The solid lines give the results calculated with parameters determined by adjusting to experimental single-particle levels in actinide nuclei, and the dashed lines those determined from ^{208}Pb. The lower part of the figure shows the modified-liquid-drop energy and the total energy (liquid-drop+pairing+shell energies) corresponding to these two sets of parameters. As seen, no secondary minimum is obtained in the total energy.

interpretation in turn seemed to imply a $|\beta|$ of 0.27 for ^{185}Hg and of 0.29 for ^{183}Hg, provided that $|\beta| = 0.15$ for ^{187}Hg. Such a large deformation would seem to imply the existence of a well-developed rotational structure for ^{183,185}Hg and most likely for ^{184}Hg. By studying the α-decay of the unusual nucleus ^{188}Pb, Hornshøj *et al.* [6]) were able to supply what appeared as strong evidence against this alternative explanation by setting very low limits for a possible α-branch to any rotational state below 500 keV for a completely unhindered decay. Any hindrance affecting a 2^+ branch implies a lower limit, as pointed out by the authors. The authors of ref. [6]) speculated that the exceedingly proton-rich nucleus ^{184}Hg might indeed be a bubble nucleus. For conserved nuclear density this explanation would imply a ratio of inner to outer radius of about 30 %. Subsequently, however, a rotational type band was observed in ^{184}Hg by the authors of ref. [7]). The corresponding spectrum is, for low-I, transitional; but for higher I, a good rotor characterized by very large B(E2) values.

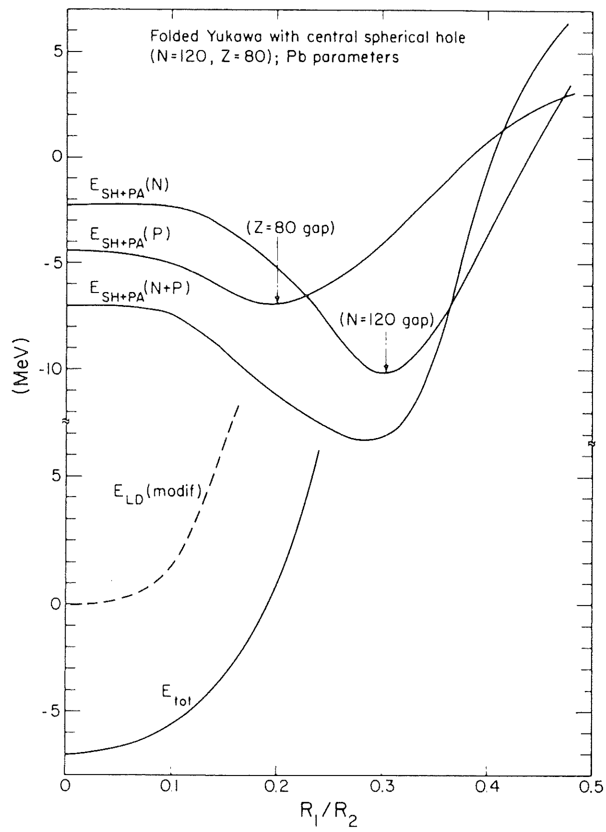

Fig. 4. Analogous to fig. 3 but for ^{200}Hg calculated with the Pb parameters. Note the deep minimum in the neutron and proton shell+pairing energy at $R_1/R_2 = 0.3$. In the lower part of the figure (see furthermore fig. 6) the modified-liquid-drop energy and the total potential energy are exhibited.

2. Calculations for bubble nuclei

To further investigate the case of the nucleus ^{184}Hg, for which this puzzling experimental evidence exists, calculations for ^{184}Hg as well as for ^{200}Hg have been performed with two improvements relative to the calculation of ref. [1]. The results are displayed in figs. 3–7. First, we have used the folded-Yukawa [8] type of potential which is generated by folding a Yukawa function over a uniform sharp-surface square-well potential defined by its inner radius R_1 and its outer radius R_2. In this way R_1 and R_2 are well defined and for the limit $R_1/R_2 = 0$ the usual homogeneous-sphere potential is recovered. The range of the Yukawa function, which specifies the surface diffuseness of the potential, and the spin-orbit interaction strengths are deter-

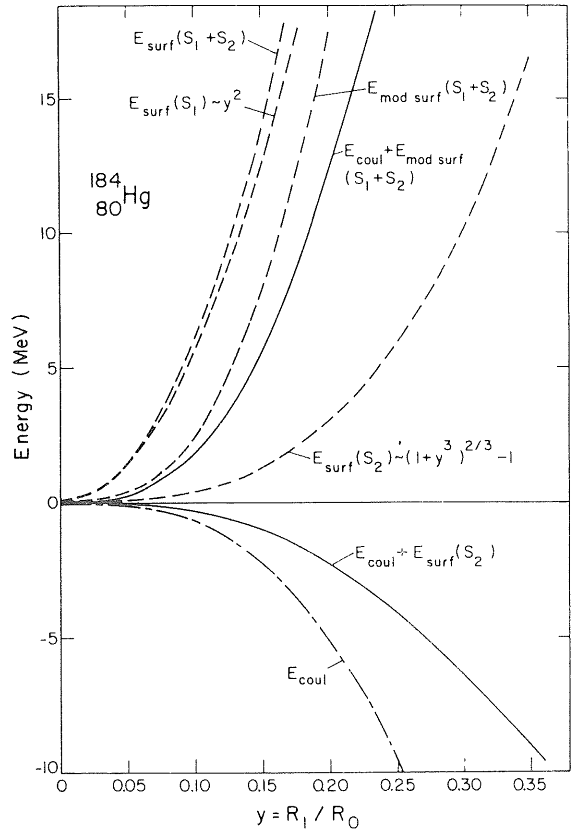

Fig. 5. Different macroscopic contributions for ^{184}Hg. For the normal surface energy note first the contribution from the inner surface S_1 rising as y^2, where $y = R_1/R_0$, R_0 being the radius of the homogeneous sphere. As $R_2^3 - R_1^3 = R_0^3$, the ratio R_1/R_2 is very close to R_1/R_0 for small values of R_1/R_2. Of less importance is $E_{surf}(S_2)$ for the outer surface. In fact, this latter function does not quite compensate the fall-off with y of the Coulomb contribution E_{Coul}, but would lead to an instability in the liquid-drop energy if the inner surface were neglected. The inner surface contribution is considerably weakened for the modified surface energy, where the finite range of the nuclear force is taken into account [10]. Still the total modified surface energy rises steeply with y. This is the case also when the Coulomb contribution is added (total modified-liquid-drop energy).

mined from adjustments to experimental single-particle levels in actinide and rare-earth nuclei [9]). We also use an alternative set of parameters [8]) obtained from adjustments to experimental single-particle levels in ^{208}Pb.

A second improvement in the present calculations relative to those of ref. [1]) is that we take into account the correction that arises from the finite range of the nuclear force [10]). This correction weakens the contribution to the usual surface energy, in particular from the inner surface (which is found to rise sharply with R_1/R_0; see fig. 5), by an order of magnitude for small R_1/R_0, R_0 being the radius of the homogeneous spherical nucleus.

In this way we obtain, as functions of R_1/R_2, the single-particle levels shown in figs. 1 and 2. They have been calculated with the folded-Yukawa potential using the Pb parameter choice. (The "actinide-parameter" choice gives very similar level diagrams.) These figures resemble largely fig. 1 or ref. [1]) with the improvement that the

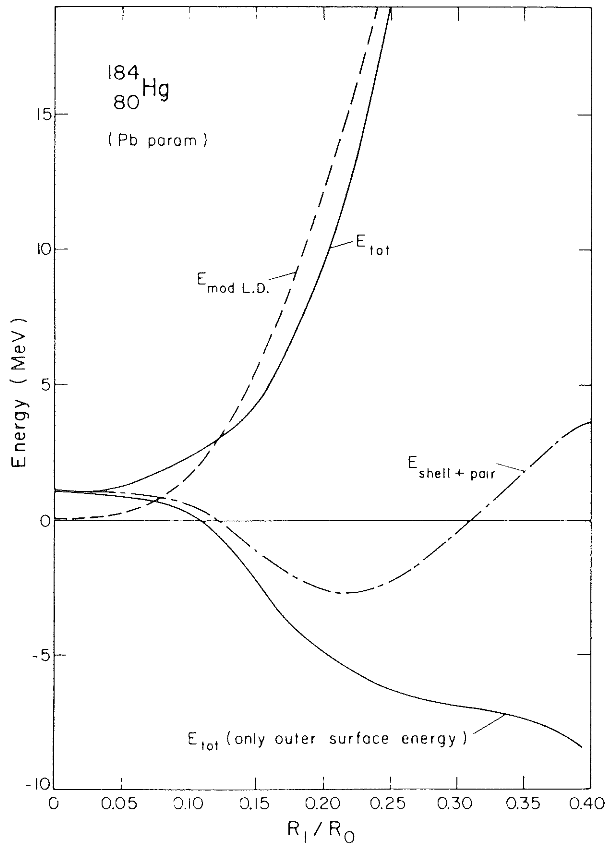

Fig. 6. For ^{184}Hg the quantity $E_{shell+pair}$ is plotted as a function of R_1/R_0. When added to the modified-liquid-drop energy as a function of R_1/R_0 the total energy E_{tot} is found to exhibit no minimum beyond that at $R_1/R_0 = 0$. Finally, the limiting case of only an outer surface energy added to the Coulomb and shell + pairing energies shows a clear instability to a blow-up.

normal homogeneous-sphere case is reproduced at the left edge of our diagrams. Both the separate shell and pairing effects for protons and neutrons and their sum are plotted in figs. 3 and 4 for ^{184}Hg and ^{200}Hg, respectively. For ^{184}Hg the maximum negative shell effects for protons is associated with $R_1/R_2 = 0.2$ while the $N = 104$ neutron shell effect has an extremum at $R_1/R_2 \approx 0.5$. Thus the shell effects for ^{184}Hg work largely against each other. The resulting shell+pairing energy minimum appears at $R_1/R_2 = 0.2$ and is only 3 MeV deep. For almost any version of the added macroscopic energy a secondary minimum can almost be ruled out in the ^{184}Hg case. The different macroscopic contributions are analyzed in fig. 5. From this figure it is apparent that in the normal version of the liquid-drop model the contribution from the inner surface rises exceedingly fast. For small values of R_1/R_0, when, due to the surface diffuseness, the bubble interior is substantially filled with matter, the treatment of the inner surface is a delicate problem. The method that we use for

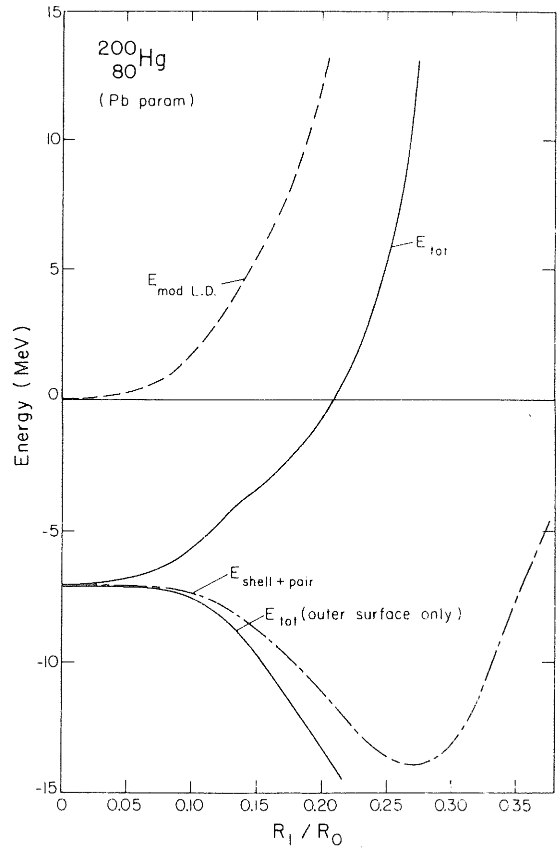

Fig. 7. Analogous to fig. 6 but for ^{200}Hg. Here the shell+pairing function shows stronger fluctuations with R_1/R_0 than in fig. 6. The shell fluctuations are still not strong enough to lead to a real secondary minimum in the total energy unless the internal surface energy is strongly weakened beyond that of the modified-liquid-drop model.

the calculation of the surface energy [10]) is aimed at accounting for this diffused matter distribution and for the finite range of nuclear forces. An interesting limit is obtained by assuming zero surface energy for the inner surface. In this unrealistic case (see figs. 5–7) the sum of surface and Coulomb energies decreases with increasing R_1/R_0.

Although some doubt may be cast on the applicability of the Strutinsky-Swiatecki method to this entire problem, it appears reasonably safe to say, in view of the weak total shell effects, that *^{184}Hg is not a bubble nucleus.* On the other hand, for ^{200}Hg the neutron and proton shell contributions occur coherently. As seen from fig. 7, the shell+pairing energy gain is about 7 MeV from $R_1/R_0 = 0$ to $R_1/R_0 \approx 0.27$. Even with the modified liquid-drop term, this is not enough to ensure a stable secondary minimum. The calculations of Davies *et al.* [4]) give here a central depression extending out to $R_1/R_0 = 0.25$ to 0.30. The ratio in question and in particular R_1 is less well defined in their case as the central matter density is of the order of 50 %. One should also note that these authors calculate a rms charge radius of 5.20 fm for ^{200}Hg as against 5.23 fm for ^{208}Pb, which amounts to only a 1.5 % increase in $\langle r^2 \rangle$ for ^{200}Hg relative to a scaled ^{208}Pb nucleus.

It thus seems fair to conclude that neither ^{184}Hg nor ^{200}Hg, whether treated according to the Strutinsky method or in terms of HF calculations, has enough of a "bubble" to provide an explanation for the finding of Bonn *et al.* [5]).

3. An alternative explanation

Rather strong evidence that ^{181}Hg, ^{183}Hg and ^{185}Hg are all normally prolately deformed nuclei comes from the following experimental and theoretical observations. Strutinsky type calculations of Faessler *et al.* [11]) based on a Woods-Saxon single-particle potential predict ^{187,189}Hg to be weakly oblate and ^{185,183}Hg to be prolate. Hartree-Fock calculations by Cailliau *et al.* [12]) also give an oblate to prolate shift for Hg isotopes going from $N = 188$ to $N = 186$. Equilibrium calculations in terms of the modified-oscillator model [13]) are in agreement with these results. However, as discussed below some modifications are brought about by a generalisation in the treatment of the pairing interaction.

Experimentally the same spin, $\frac{1}{2}$, is measured for all of these Hg isotopes, ^{181,183,185}Hg, and the measured magnetic moments are nearly the same for all of the three isotopes. This strongly suggests that the same orbital is involved. Actually the orbital [521$\frac{1}{2}$] appearing on the prolate side (see fig. 8) gives $\mu \approx 0.4$ n.m. for $\varepsilon \approx 0.2$ [refs. [14,15])] under the usual assumption that $g_s = 0.6\, g_s^{\mathrm{free}}$ while the measured magnetic moments fall between 0.45 and 0.51. On the other hand, on the oblate side no proper orbital giving a magnetic moment of this magnitude is available. Faessler *et al.* argue that probably the zero-point vibrations change in amplitude from the oblate ^{187}Hg to the prolate ^{181,183,185}Hg and by enough to explain the shift in $\langle r^2 \rangle$ from $A = 187$ to $A = 185$, in addition to what can be ascribed to a change in $|\beta|$ or $|\varepsilon|$ of the potential energy minima. The latter shift is responsible for most of the effect, however.

We have here investigated the effect of quadrupole pairing [16,17]) on the potential-energy surface. One should notice a remarkable feature apparent from fig. 9, where the single-proton levels are shown as functions of ε ($\varepsilon_4 = 0$). In particular, examine the levels at $\varepsilon \approx 0.2$, which distortion corresponds to the potential-energy minimum with inclusion of monopole pairing for ^{184}Hg. Just above the Fermi surface there occurs at this distortion a region of remarkably frequent crossings of down-coming polar orbitals and up-sloping equatorial ones. This is a situation where the recently introduced modification of the usual monopole pairing assumption is expected to be important. The simplest generalisation is that of quadrupole pairing [16,17]). This theory allows for the fact that the matrix element representing the scattering of a pair

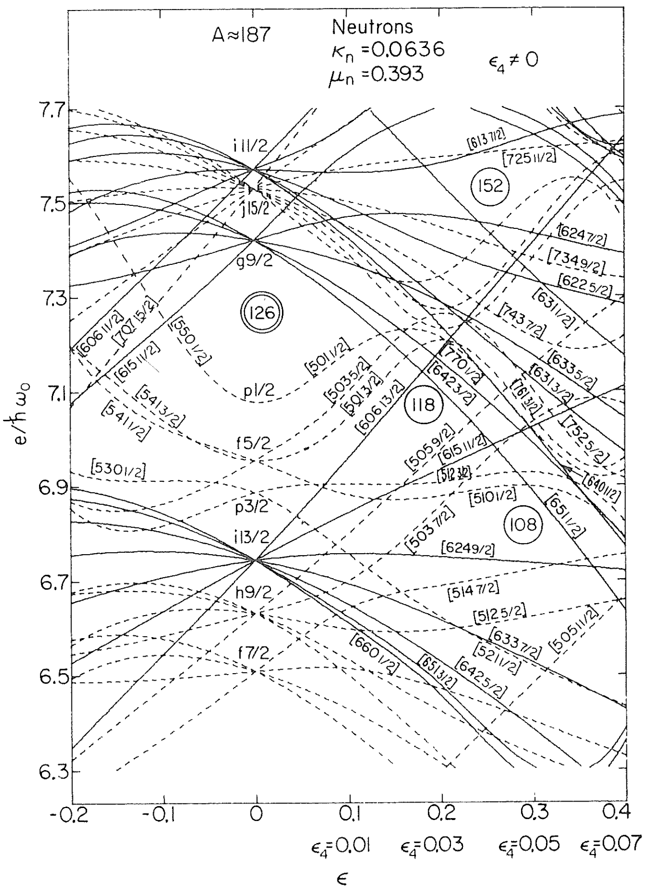

Fig. 8. Single-neutron levels in the heavy rare-earth region. Note that [521½] appears as the $N = 99$, 101, 103, and 105 orbital between $\varepsilon = 0.25$ and $\varepsilon = 0.15$ due to crossings with other orbitals.

between oblate and prolate orbitals is much weaker than the matrix elements connecting only prolate or only oblate orbitals. In the quadrupole pairing picture one expects a relative weakening of the total pair correlation energy around $\varepsilon = 0.2$ compared with what the high level density at first appears to imply. The introduction of quadrupole pairing thus gives to the unmodified potential-energy surface a trend away from this distortion. This same effect is to some extent obtained by the authors of ref. [12]) by their recipe of having Δ instead of G constant with deformation. This will also lead to smaller pairing correlations in the region of high level density around $\varepsilon = 0.2$. As discussed in the following, we find for $^{182, 184, 186}$Hg larger distortions where polar orbitals occur near the Fermi surface. The change in equilibrium ε leads to larger $\langle r^2 \rangle$, corresponding to the fact that $N = 4$ and 5 orbitals are replaced with $N = 6$ and 5 ones. With the larger equilibrium distortion the effect is somewhat magnified by the large smearing over many levels due to the quadrupole pairing for

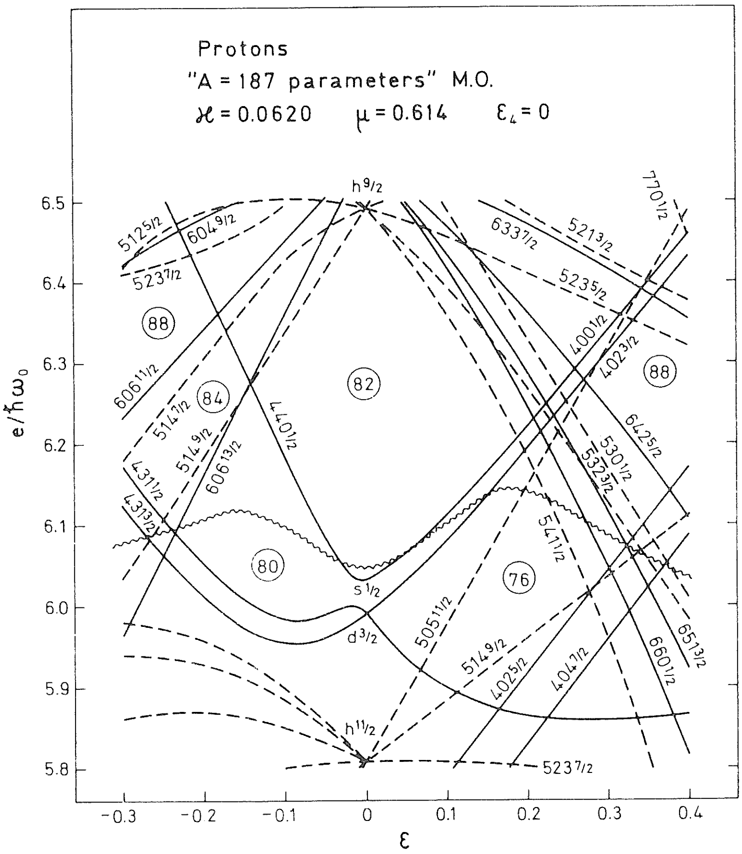

Fig. 9. Single proton levels in the modified-oscillator model in the heavy rare-earth region. Note the crossing of several equatorial and polar orbitals near $\varepsilon = 0.2$ for $Z = 80$. The Fermi level for ^{184}Hg, in the case of ordinary monopole pairing, is indicated by the thin wiggled line.

the case of orbitals of similar type, i.e. of similar quadrupole moments. We have carried out calculations in the present investigation similar to those of ref. [17]). Thus we have assumed that the pairing Hamiltonian may be written

$$H_P = -g_0 P_0^+ P_0 - g_2 P_2^+ P_2,$$

where

$$P_0^+ = \sum a_\nu^+ a_{\bar{\nu}}^+, \qquad P_2^+ = \sum q_{\nu\nu} a_\nu^+ a_{\bar{\nu}}^+.$$

An important problem is how the quadrupole matrix elements $q_{\nu\nu}$ are to be defined when a large region of distortions is included. We have used a definition which is a generalisation of that used in ref. [17]):

$$q_{\nu\nu} = \langle \nu | \sqrt{\tfrac{16}{5}\pi} \rho^2 Y_{20}(\theta_t, \phi_t) | \nu \rangle / \langle \nu | \rho^2 | \nu \rangle,$$

where ρ is the radius vector and θ_t, ϕ_t are the angles in the stretched coordinate system [13]). This definition results in a constant "asymptotic" limit for large distortions. Even this generalisation of the quadrupole pairing force leads to a systematic increase of the pairing with distortion. The gross part of this surface-pairing type effect should probably be considered as already included in the surface energy employed in the liquid-drop model. With the aim of eliminating most of the smooth contribution from the quadrupole pairing we have superimposed the auxiliary requirement

$$g_2 (q_{\nu\nu}^2)_{\text{average}} = g_0 k,$$

where the average is taken over all levels included in the pairing calculation according to the prescription of ref. [13]). We have chosen $g_0 = 0.95\, \overset{0}{g}_0$ and $k = 0.6$, where $\overset{0}{g}_0$ is the value used in the monopole pairing calculations without inclusion of quadrupole pairing [13]). This value of k makes the quadrupole pairing strength of the same order (somewhat smaller) than the strength used in ref. [17]) for a specific deformation.

The results of the calculations, as far as the equilibrium distortions are concerned, are shown in fig. 10, which refers to three calculational cases, namely:

(i) Monopole pairing with only ε-distortion.
(ii) Monopole pairing with ε_4 included.
(iii) Both ε_4 and quadrupole pairing included.

In the latter case the calculations were initially performed with quadrupole pairing but with $\varepsilon_4 = 0$. The effect of ε_4 was subsequently added. The latter was then assumed to be equal to the ε_4 contribution given by the energy difference between cases (i) and (ii). Thus, for ^{184}Hg the resulting minimum with all effects included is found at $\varepsilon = 0.27$ which represents a substantial increase in distortion relative to case (i) ($\varepsilon = 0.20$). The rotation-like sequence of levels reported for ^{184}Hg (ref. [7])) and ^{186}Hg (ref. [18])) shows a good rotational energy spacing but first for the levels above 6^+. Indeed for ^{184}Hg the $B(\text{E2}; 6 \rightarrow 4)$ appears to imply $\varepsilon \approx 0.25$. This may be taken to give empirical evidence for a picture with a shallow potential-energy minimum but with the minimum distortion corresponding to a large value of the quadru-

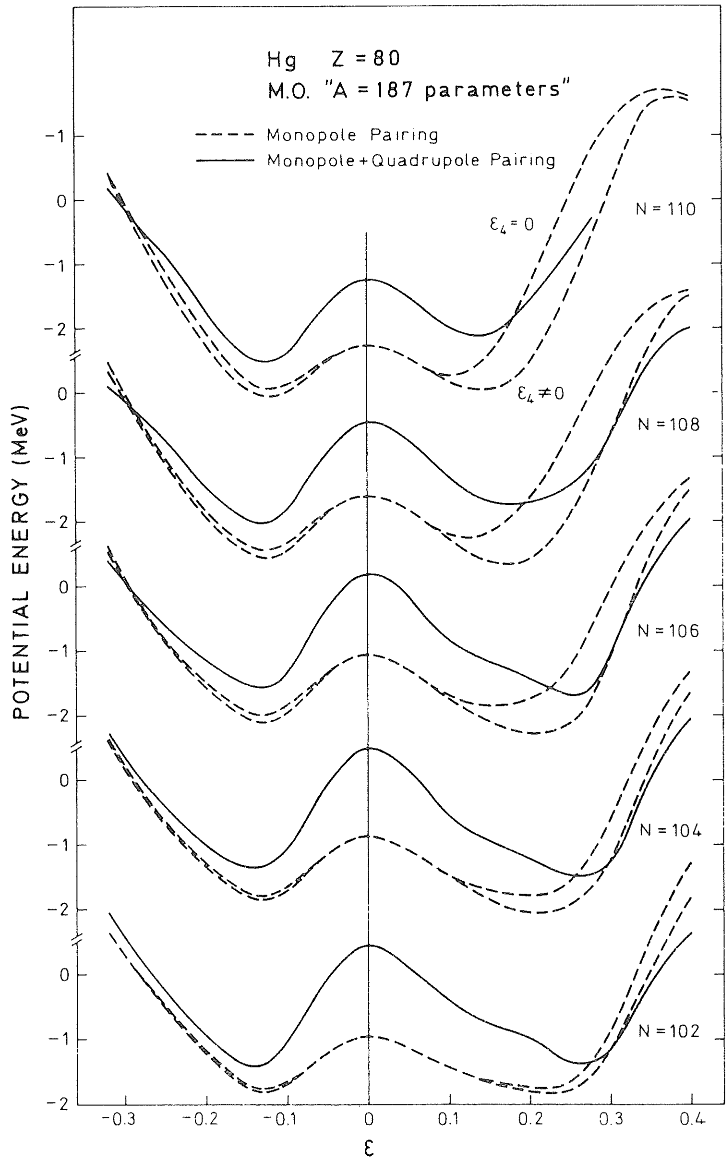

Fig. 10. Potential energy, as a function of ε, for $^{182-190}$Hg. The dashed lines correspond to ordinary monopole pairing, where ε_4 is assumed equal to zero, and alternatively where a minimisation with respect to ε_4 is carried out. The solid lines correspond to the case that both monopole and quadrupole pairing is included. Also ε_4 is included in this latter case; however, we have assumed that the effect of ε_4 is the same as in the monopole pairing case. Note in particular the large increase in the ε-value of the prolate minimum when going from ^{188}Hg to ^{186}Hg.

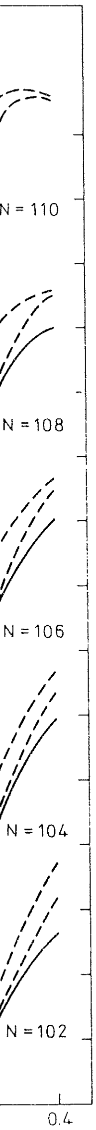

hed lines correspond to
d alternatively where a
nd to the case that both
s latter case; however, we
se. Note in particular the
m ^{188}Hg to ^{186}Hg.

pole moment. This finding is therefore grossly consistent with the potential energy calculated here (fig. 10).

From the corresponding single-particle wave functions we have evaluated $\langle r^2 \rangle$ for the equilibrium shapes assuming $\varepsilon_4 = 0$ when evaluating the wave functions. The results are plotted in fig. 11, where the crosses refer to the prolate minimum and the circles to the oblate minimum for each nucleus. Also the energy difference in the cases considered is plotted in fig. 11. The trend indicated in these calculations, as in most others, is clearly from oblate to prolate with decreasing N in this region.

The shift from oblate to prolate equilibrium, so that nuclei with $A \geqq 188$ are oblate and nuclei with $A \leqq 186$ are prolate is associated with a large change in $\langle r^2 \rangle$. Our calculations thus show that the change of shape is associated with an increase in

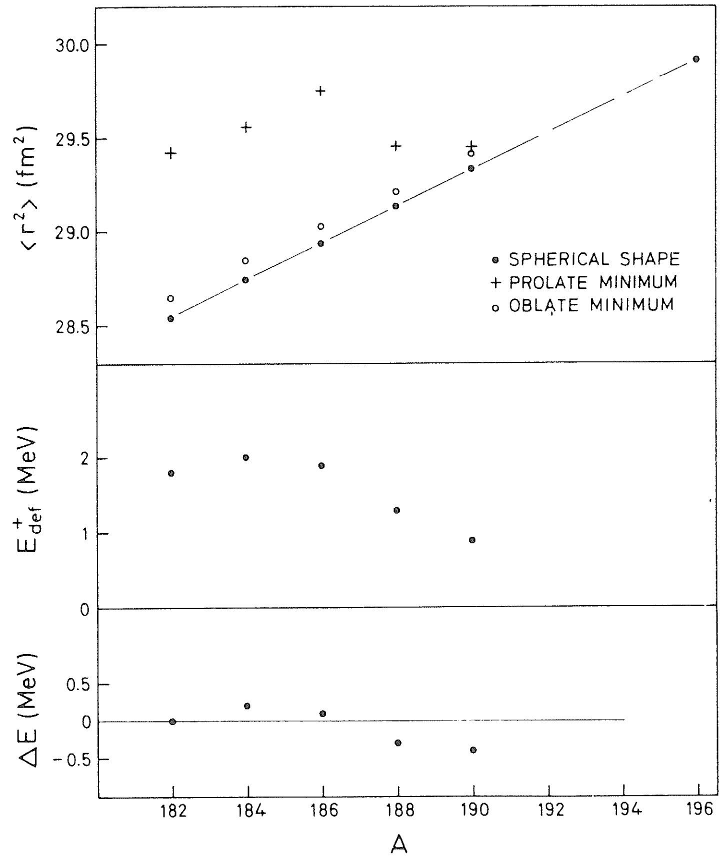

Fig. 11. The upper part of the figure shows the calculated value of $\langle r^2 \rangle$ corresponding to spheri shape, oblate minimum and prolate minimum, respectively. The ε-values of the minima are the corresponding to the solid lines in fig. 10. In the middle part the depth of the prolate minimum E^+_d measured relative to the spherical shape energy, is exhibited and in the lower part the prolate-obl energy difference, ΔE, is shown. If ΔE is larger than zero, the prolate minimum is deeper than oblate one.

$\langle r^2 \rangle$ of about 2.5%. This increase accounts for practically all of the observed radial isomeric shift.

A final treatment of the latter problem will ultimately have to include a complete dynamical calculation with a distortion dependent mass tensor (some possible effects from this source have been discussed by Dickmann and Dietrich [19]). However, in these dynamical calculations quadrupole pairing should enter both on the potential-energy side, as has been made very apparent from this study, and on the mass tensor side.

The realization of the large contribution from quadrupole pairing in this particular region of nuclei receives additional support by the observation of the anomalously low-lying (470 keV) 0^+ state in ^{186}Pt reported by Foucher *et al.* [20]).

We thus conclude that the increase in $\langle r^2 \rangle$ is not due to radial shell structure effects but rather to effects of change in distortion, for which change quadrupole pairing is eminently important.

We are grateful to Drs. C. Y. Wong, F. Stephens and R. Diamond for communicating their results prior to publication, to Drs. D. Bès, R. Broglia, B. Mottelson, K. Neergård, B. Nilsson, P. Vogel and E. Volkov for discussions on the quadrupole pairing phenomenon, and finally to Dr. P. G. Hansen for generous advice on the entire light Hg problem.

References

1) C. Y. Wong, Phys. Lett. **41B** (1972) 446
2) J. A. Wheeler, unpublished (prior to 1950)
3) W. J. Swiatecki, unpublished (1968)
4) K. T. R. Davies, C. Y. Wong and S. J. Krieger, Phys. Lett. **41B** (1972) 455;
K. T. R. Davies, S. J. Krieger and C. Y. Wong, Nucl. Phys. **A216** (1973) 250;
X. Campi and D. W. L. Sprung, Phys. Lett. **46B** (1973) 291
5) J. Bonn, G. Huber, H. J. Kluge, L. Kugler and E. W. Otten, Phys. Lett. **38B** (1972) 308; 5th Annual Conf. on atomic spectroscopy (EGAS), Lund, 1973;
J. Bonn, G. Huber, H. J. Kluge, U. Kopf, L. Kugler and E. W. Otten, Phys. Lett. **36B** (1971) 41
6) P. Hornshøj, P. G. Hansen, B. Johnson, A. Lindahl and O. B. Nielsen, Phys. Lett. **43B** (1973) 377
7) N. Rud, D. Ward, H. R. Andrews, R. L. Graham and J. S. Geiger, Phys. Rev. Lett. **31** (1973) 1421
8) M. Bolsterli, E. O. Fiset, J. R. Nix and J. L. Norton, Phys. Rev. **C5** (1972) 1050
9) P. Möller, S. G. Nilsson and J. R. Nix, to be published
10) H. J. Krappe and J. R. Nix, in Proc. Third IAEA Symp. on the physics and chemistry of fission, Rochester, New York, Aug. 13–17, 1973, to be published
11) A. Faessler, U. Götz, B. Slavov and T. Ledergerber, Phys. Lett. **39B** (1972) 579
12) M. Cailliau, J. Letessier, H. Flocard and P. Quentin, Phys. Lett. **46B** (1973) 11
13) S. G. Nilsson, C. F. Tsang, A. Sobiczewski, Z. Szymański, S. Wycech, C. Gustafsson, I. L. Lamm, P. Möller and B. Nilsson, Nucl. Phys. **A131** (1969) 1
14) P. G. Hansen, private communication (1973)
15) I. L. Lamm, Nucl. Phys. **A125** (1969) 504
16) R. E. Griffin, E. D. Jackson and E. Volkov, Phys. Lett. **36B** (1971) 281
17) D. R. Bès and R. Broglia, Phys. Rev. **C3** (1971) 2349;
D. R. Bès, R. Broglia and B. Nilsson, Phys. Lett. **40B** (1972) 338
18) D. Proetel, R. Diamond, P. Kienle, J. R. Leigh, K. H. Maier and F. Stephens, Proc. Int. Conf. on nuclear physics, vol. 1, Munich, 1973 (North-Holland, Amsterdam, 1973) p. 319
19) F. Dickmann and K. Dietrich, Z. Phys. **263** (1973) 211
20) B. Erdal, M. Finger, R. Foucher, J. P. Husson, J. Jastrzebski, A. Johnson, N. Perrin, R. Heck, R. Regal, P. Siffert, G. Astner, A. Kjelberg, P. Patzelt, A. Höglund and S. Malmskog, CERN 70-29 (1970) p. 1013